Journal of the Nigerian Association of Mathematical Physics
Volume27, (July, 2014), pp179 – 188
© J. of NAMP

MHD Stagnation Point Flow with Heat Transfer Over a Permeable Surface in the Presence of Heat Generation

Okedoye A. M.[1], Areo A. O.[1] and Asibor R. E.[2]

[1]Department of Mathematics & Computer Science, Federal University of Petroleum Resources, P.M.B. 1221, Effurun, Delta State, Nigeria.
[2]Department of Physical Sciences, Wellspring, Benin City, Nigeria

Abstract

This paper studied the steady laminar two – dimensional stagnation point flow of an incompressible viscous electrically conducting fluid at stagnation point with heat transfer. Uniform magnetic field is applied externally normal to the plane of the wall. Employing similarity transformations, the governing partial differential equations are transformed into ordinary differential equations. This were solved in non – dimensional state numerically using central differences for the derivatives and Thomas algorithm for the solution of the set of discretized equations in the infinite domain $0 < \eta < \infty$. ***A finite domain in the η-direction was used instead with η chosen large enough to ensure that the solutions are not affected by imposing the asymptotic conditions at a finite distance. Numerical results for the dimensionless velocity profiles, the temperature profiles, the local friction coefficient and the local Nusselt number are presented for various parameters. These results are presented to illustrate the influence of the Hartmann number, suction parameter, heat absorption coefficient and, thermal and mass Grashof numbers. The effects of various emerging parameters are seen on the velocity and temperature fields. The values of the wall shear stress are also tabulated for different cases.***

Keywords: Magneto hydrodynamic fluid, Thomas algorithm, Heat transfer; Boundary layer; Stagnation point, Generative reactions.

1.0 Introduction

In fluid dynamics, a stagnation point is a point in a flow field where the local velocity of the fluid is zero. Stagnation points exist at the surface of objects in the flow field, where the fluid is brought to rest by the object. A stagnation point occurs whenever a flow impinges on a solid object. Usually there are other important features of the flow.

Magnetohydrodynamics has attracted the attention of a large number of scholars due to its diverse applications. In astrophysics and geophysics, it is applied to study the stellar and solar structures, matter, radio propagation through the ionosphere etc. in engineering it find its application in MHDpumps and generators, convection in porous media has applications in geo-thermal energy recovery, oil extraction, thermal energy storage and flow through filtering devices.

In the history of fluid dynamics, considerable attention has been given to the study of 2-D stagnation point flow. Hiemenz [1] derived an exact solution of the steady flow of a Newtonian fluid impinging orthogonally on an infinite flat plate. Stuart [2], Tamada [3] and Dorrepaal [4] independently investigated the solutions of a stagnation point flow when the fluid impinges obliquely on the plate. Beard and Walters [5] used boundary-layer equations to study two-dimensional flow near a stagnation point of a viscoelastic fluid. Dorrepaal et al [6] investigated the behaviour of a viscoelastic fluid impinging on a flat rigid wall at an arbitrary angle of incidence. Labropulu et al. [7] studied the oblique flow of a viscoelastic fluid impinging on a porous wall with suction or blowing. The Hiemenz flow of a Newtonian fluid in the presence of a magnetic field was first considered by Na [8] and later by Ariel [9]. Recently, Okedoye et al [10] reported MHD Flow of a Uniformly Stretched Vertical Permeable Surface under Oscillatory Suction Velocity.

The purpose of the present work is to study the steady laminar MHD flow of an incompressible viscous electrically conducting fluid at a stagnation point with heat transfer, in the presence of heat generation. The fluid is acted upon by an external uniform magnetic field and a uniform suction or injection directed normal to the plane of the wall.

Corresponding author: Okedoye A. M.E-mail:dele.mikeoke@gmail.com,Tel.: +2348035688453 & 08034331960 (A.R.E)

2. 0 Formulation of the Problem

Consider the two-dimensional stagnation point flow of a viscous incompressible electrically conducting fluid impinging perpendicular to a permeable plane directed along the *x*-axis. This is an example of a plane potential flow which arrives from the entire space above the plate and impinges on a flat wall placed at *y*=0, divides into two streams on the wall and leaves in both directions. Here, (*u*, *v*) are the components of velocity at any point (*x*, *y*) for the viscous flow, whereas (*U*, *V*) are the velocity components for the potential flow. A uniform magnetic field *B*o and a uniform suction or injection with a transpiration velocity at the boundary of the plate are given by $-v_0$ for suction and v_0 for injection are applied normal to the plane.

Then, for the two-dimensional steady state flow, the continuity and momentum equations, using the usual boundary layer approximations [11] and by introducing Lorentz force, reduce to:

$$\frac{\partial u}{\partial x}+\frac{\partial v}{\partial y}=0, \tag{1}$$

$$u\frac{\partial u}{\partial x}+v\frac{\partial v}{\partial y}=U\frac{dU}{dx}+\upsilon\frac{\partial^2 u}{\partial y^2}+\frac{\sigma B_0^2}{\rho}\left(U(x)-u\right)+\frac{g\beta_\tau}{\rho}\left(T-T_\infty\right)+g\beta_c\left(C-C_\infty\right)=0, \tag{2}$$

where ρ, υ, and σ are, respectively, the density, the kinematic viscosity, and the electric conductivity of the fluid and *U*(*x*) is the horizontal component of the inviscid potential flow velocity above the boundary layer formed over the plate surface. The boundary conditions for the velocity problem, assuming the absence of magnetic field in the potential flow region, are given by:

$$u(x,0)=0,\ v(x,0)=-v_0\text{, for suction or } v(x,0)=v_0 \text{ for injection,} \tag{3a}$$

$$u(x,\infty)=U(x)=ax,\ v(x,\infty)=v(y)=-ay,\ p(x,\infty)=p_0-\frac{\rho a^2}{2\left(x^2+y^2\right)}, \tag{3b}$$

where '*a*' is a constant. The temperature distribution can be found from the energy equation which may be written as (neglecting the dissipation),

$$\rho c_p\left(u\frac{\partial T}{\partial x}+v\frac{\partial T}{\partial y}\right)=k\frac{\partial^2 T}{\partial y^2}+Q\left(T-T_\infty\right), \tag{4}$$

where*T*is the temperature of the fluid, c_p is the specific heat capacity at constant pressure of the fluid, and *k* is the thermal conductivity of the fluid. The boundary conditions for the temperature problem are given by:

$$T(x,0)=T_w,\ T(x,\infty)=T_\infty, \tag{5}$$

Also the reactant concentration distribution equation can be written as

$$\rho\left(u\frac{\partial C}{\partial x}+v\frac{\partial C}{\partial y}\right)=D\frac{\partial^2 C}{\partial x^2}-A_0\left(C-C_\infty\right) \tag{6}$$

Where*C*is the concentration of the chemical species, *D* is mass diffusion coefficient at constant pressure, and A_0 is the chemical reactant parameter of the fluid. The boundary conditions for the reactant problem are given by:

$$C(x,0)=C_w,\ C(x,\infty)=C_\infty \tag{7}$$

By introducing the following dimensionless variables and parameters

$$\eta=\sqrt{\frac{a}{\upsilon}}y,\ u(x,y)=axf'(\eta),\ v(x,y)=-\sqrt{a\upsilon}\,f(\eta),\ g(\eta)=\frac{T-T_\infty}{\left(T_w-T_\infty\right)},\ h(\eta)=\frac{C-C_\infty}{\left(C_w-C_\infty\right)},$$

The derivatives become,

$$\frac{\partial u}{\partial x}=af'\ \frac{\partial u}{\partial y}=ax\sqrt{\frac{a}{\upsilon}}f'',\ \frac{dU}{dx}=a,\ \frac{\partial^2 u}{\partial y^2}=ax\left(\sqrt{\frac{a}{\upsilon}}\right)^2 f''',$$

$$\frac{\partial v}{\partial y}=-af',\ A=f(0)=\pm\frac{v_0}{\sqrt{a\upsilon}},$$

Where*A*is the suction parameter; *A*>0 is for suction and *A*<0 is for injection, and the governing Equations (1) to (7) reduce to:

$$f''' + ff'' + M^2(1 - f') - f'^2 + Gr\tau\theta + Grch + 1 = 0 \quad (8)$$

$$\theta'' - \Pr(f' - f)\theta' + \Pr\phi\theta = 0 \quad (9)$$

$$h'' + Sc(h'f - hf') - \gamma Sch = 0 \quad (10)$$

$$\left.\begin{aligned} &f(y) = \pm\alpha,\ f'(y) = 0,\ \theta(y) = 1,\ h(y) = 1 \quad at\ y = 0 \\ &f(y) \to \beta\eta\ ,\ f'(y) \to 1,\ \theta(y) \to 0,\ h(y) \to 0\ at\ y \to \infty \end{aligned}\right\} \quad (11)$$

here primes denote differentiation with respect to η.

where $\alpha = \frac{\pm v_0}{\sqrt{a\upsilon}} = A,\quad \beta = \sqrt{\frac{\upsilon}{a}},\ Sc = \frac{\rho\upsilon}{D},\ \Pr = \frac{\mu c_p}{k},\ \phi = \frac{Q}{a\mu c_p},$

$$Gr\tau = \frac{g\beta_\tau}{\rho a^2}(T_w - T_\infty),\ Grc = \frac{g\beta_c}{\rho a^2}(C_w - C_\infty),\ \gamma = \frac{A_0}{a\rho}$$

The flow Equations (8) to (10) subject to boundary conditions (11) are solved numerically using finite differences. A shooting technique is first applied to convert the higher order derivatives to a system of first order differential equations.

The solution for the non-magnetic case is chosen as an initial guess and the iterations using Euler scheme are continued till convergence within prescribed accuracy is achieved, with the corrections incorporated in subsequent iterative steps until convergence, which is used to obtain the values of our initial guesses. Finally, the resulting guesses together with the system was solved using generalized Thomas' algorithm.

The system of equations has to be solved in the infinite domain $0 < \eta < \infty$.A finite domain in the η-direction can be used instead with η chosen large enough to ensure that the solutions are not affected by imposing the asymptotic conditions at a finite distance.

Grid-independence studies show that the computational domain 0<η< η∞ can be divided into intervals each of uniform step size which equals 0.02. This reduces the number of points between $0 < \eta < \eta_\infty$ without sacrificing accuracy. The value $\eta_\infty = 10$ was found to be adequate for all the ranges of parameters studied here.

3.0 Results and Discussion

In this analysis, we investigate the effect of suction $+\alpha$ injection $-\alpha$, Hartmann Number ($M \geq 0$), Thermal and mass Grashof numbers (Grt, Grc), heat source/sink coefficient ϕ and chemical reaction parameter γ. In general, for our case here, *Pr<1* which means the conduction effects exceeds viscous diffusion the thermal boundary layer is thicker than the velocity boundary layer. The study is carried out on velocity, temperature and concentration profiles.

It could be seen from figure 1 that as suction parameter reduces axial velocity *f* (η) reduces while as injection increases the axial velocity also increases. It is established the fact that decrease in suction implies increase in injection. When the injection value is kept constant, the axial velocity increases with increase in thermal Grashof number for cooling of the plate$(Grt > 0)$.

Figure 2 shows the transient velocity profiles $f'(\eta)$ for various values of Hartmann number M. The figure brings out clearly the effect of the Hartmann number M on the velocity boundary layer thickness. Increasing M decreases the velocity boundary layer.

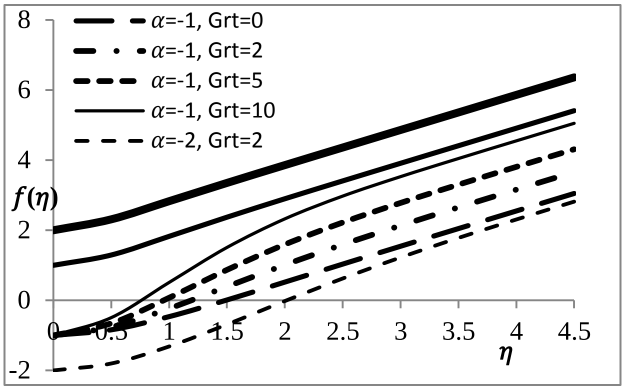

Figure 1: Axial velocity profile

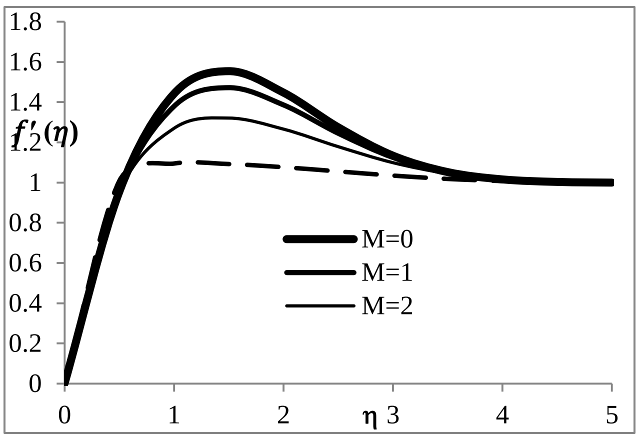

Figure 2: Transient Velocity for various values of HartmannNumber

The effect of M on $f'(\eta)$ is more pronounced for smaller values of M. It could also be deduced that very close to the surface, variation in Hartmann number is not significant until the flow approached $\eta \to 1.0$. We discovered that a maximum velocity is within the body of the fluid far away from the surface as shown by the peak in the profile (Figure 2)

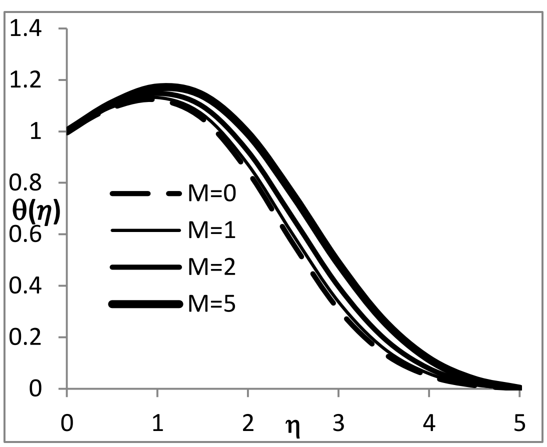

Figure 3: Temperature distributions for various values of Hartmann Number

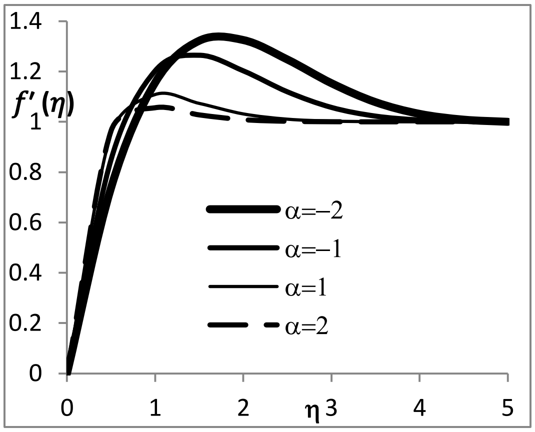

Figure 4: Variation of $f'(\eta)$ for various values of α

In Figure 3 as position ηapproaches 1.0, the effect of Hartmann number becomes significant such that increase in Hartmann number brings about increase in temperature. The temperature is maxima at the lowest velocity for highest Lorentz force. Also, it could be seen that the temperature close to the surface is higher than the surface temperature as a result of heat loss through axial temperature. At $\eta = 1.5$, increasing M from 0 to 2.0 increases the temperature by 5%, at $\eta = 2.0$, increasing M from 0 to 2.0 increases the temperature by 9% and at$\eta = 3.5$, increasing M from 0 to 2.0 increases the temperature by 43% while increase in M furtheras $\eta > 4.0$ increase in temperature reduces and decay asymptotically to 0 from $\eta = 5$.

Figure 4 show that increasing α decreases the velocity boundary layer thickness. It is also clear from Figure 4 that increasing the injection velocity increases the velocity, while increasing the suction velocity decreases the velocity. The velocity is higher close to the surface for Suction (α >0) and lower for fluid injection (α <0)close to the surface as of collision between the fluid material.

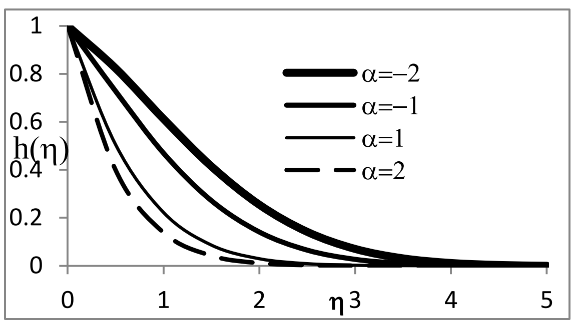

Figure 5: Concentration distributions for various values of α

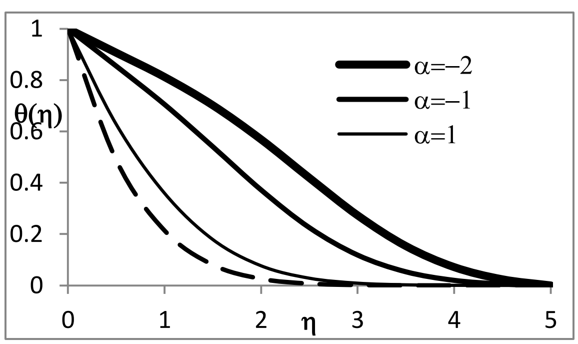

Figure 6: Temperature distributions for values of α

Figure 5 presents the concentration profile $h(\eta)$ for various values of α . The figure indicates that the species boundary layer thickness decreases as α increases. It is clear from the figure that injection increases the concentration since more reactant is being pumped in, and vice versa. For larger values of α , the concentration field decreases rapidly. The action of fluid injection is to fill the space immediately adjacent to the plate with fluid having nearly the same temperature as that of the disk.

As shown in Figure 6, the effect of fluid injection (α <0) is to decrease the heat transfer significantly by blanketing the surface with fluid whose temperature is close to T_w. Suction (α >0) has an opposite effect on the heat transfer, since fluid at near-ambient temperature is brought to the neighborhood of the surface of the plate. These effects are manifested by the progressive flattening of the temperature profile adjacent to the plate. Thus, the injected flow forms an effective insulating layer, decreasing the heat transfer from the plate. Suction, on the other hand, serves the function of bringing large quantities of ambient fluid into the immediate neighborhood of the plate surface. As a consequence of the increased heat-consuming ability of this augmented flow, the temperature drops quickly as we proceed away from the plate.

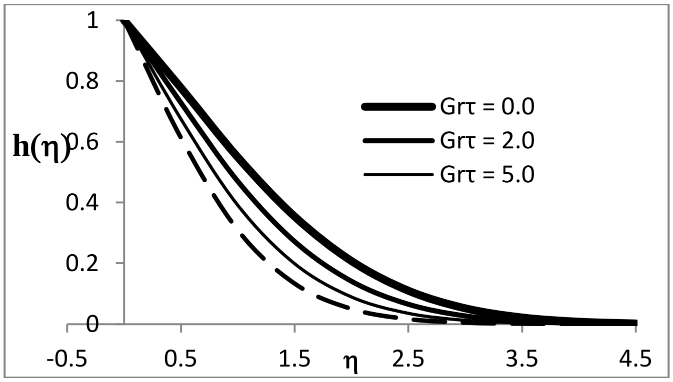

Figure 7: Concentration distributions for various values of thermal Grashof number

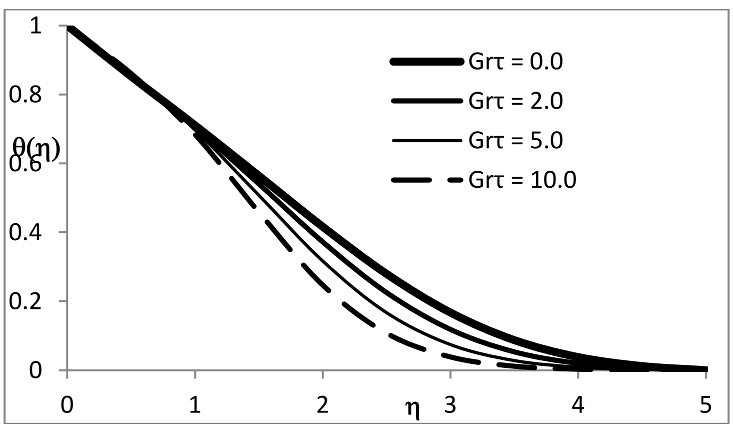

Figure 8: Temperature distributions for various values of thermalGrashof number

In Figure 7, increase in thermal Grashof number brings about decrease in concentration boundary layer. The effect on thermal Grashof number on concentration field is that as thermal Grashof number increases more reactant is being consumed.

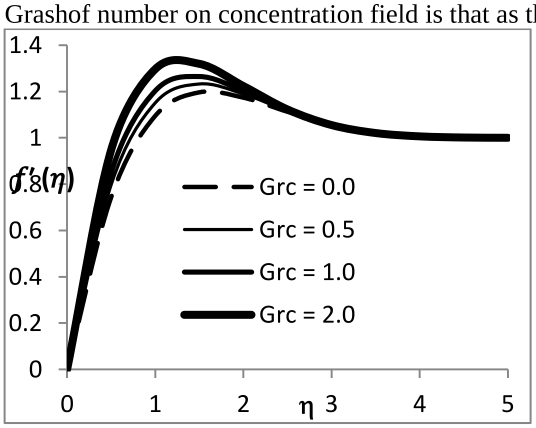

Figure 9: Velocity distributions for various values of mass Grashof number

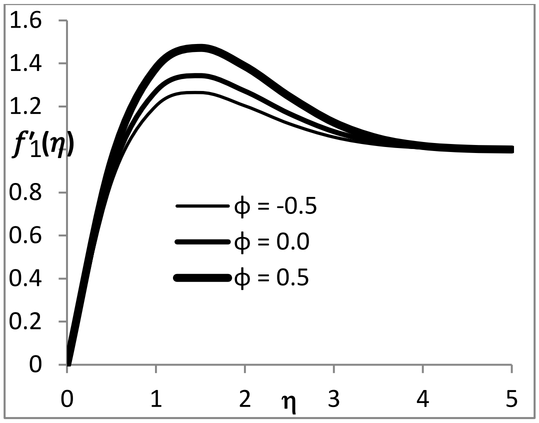

Figure 10: Velocity distributions for various values of heat source/sinkcoefficien

Figure 8 depict the effect of thermal Grashof number on transverse temperature field. Variation in thermal Grashof number for $\eta \leq 1$ is less significant until $\eta > 1$ when increase in thermal Grashof number reduces temperature boundary layer. This is shown in figure 8, as thermal Grashof number increases the temperature boundary layer reduces which make the fluid to retain more heat far away from the plate.
The effect of mass Grashof number on transient velocity $f'(\eta)$ is shown in figure 9. Consumption of more chemical species will increase the reactivity of the fluid thereby making more molecules available for the process. This in turn brings about increase in the velocity boundary layer. Increasing thermal Grashof number further from $\eta = 2.5$, variation in thermal Grashof number is not significant.

Figure 10 show the transient velocity $f'(\eta)$ profile for various values of heat generation or absorption parameter ϕ. It is clear that the effect of the ϕ on the velocity boundary layer thickness is significant close to the surface. Increasing heat absorption increases the thermal boundary layer thickness, while increase heat generation reduces the transient velocity boundary layer thickness. The effect of ϕ on $f'(\eta)$ is more pronounced for values of ϕ between $0.7 < \eta < 3.5$. It is also seen that maximum velocity occurs in the body of the fluid away from the surface within this domain.

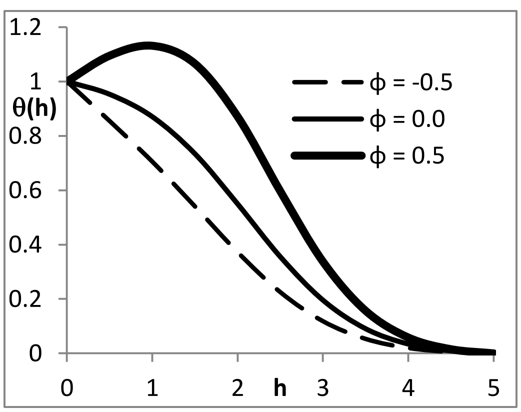

Figure 11: Temperature distributions for various values of heat source/sinkcoefficient

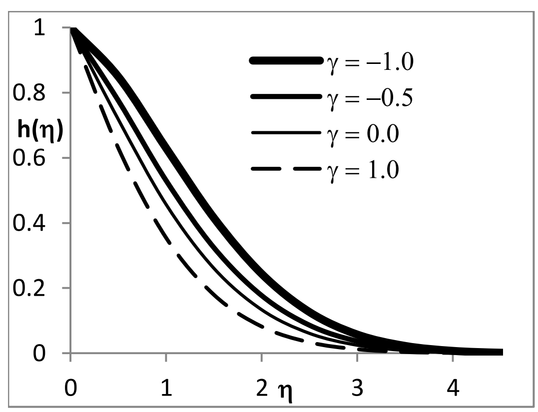

Figure 12: Concentration distributions for various values of reaction parameter

It is clear from Figure 11 that the effect of the φ on the velocity boundary layer thickness is significant, with heat absorption having maximum temperature different from the surface temperature. Increasing heat absorption decreases the thermal boundary layer thickness, while heat generation increases the thermal boundary layer thickness.

Effect of chemical reactivity on velocity, temperature and concentration field is shown in Figure 12. It should be noted here that, $\gamma < 0$ correspond to generative chemical reaction and $\gamma > 0$ correspond to destructive chemical reaction. It is observed that increase in generative chemical reaction increases the concentration distribution, while the reverse is the case for destructive chemical reaction. Furthermore the concentration is maxima at the plate, that is maximum concentration is the concentration at the surface and then decays to zero asymptotically.

4.0 Analysis of dimensionless number on the flow

We now move to examining some important fluid parameters that are of importance to this work. Such parameters include Sherwood number, Nusselt number and Skin – friction coefficient. We therefore denote and define respectively, Sherwood number and Skin – friction coefficient as [10].

$$Sh = \frac{J_\omega \, v}{(c_\omega - c_\infty) D v_\omega} = \frac{-d}{d\eta} h(0), \quad J_\omega = -D \frac{dh}{d\eta}\Big|_{\eta=0}$$

$$c_f = \frac{T_f}{\rho u_\omega v_\omega} = \frac{d^2}{d\eta^2} f(0), \quad \tau_f = \mu \frac{df}{d\eta}\Big|_{\eta=0}$$

The heat transfer at the wall is computed from Fourier's law:

$$Nu = \frac{q_\omega v}{(T_\omega - T_\infty) K v_\omega} = \frac{-d}{d\eta}\theta(0), \quad q_\omega = -K \frac{dT}{dy}\Big|_{y=0},$$

Table 1 presents the effect of the parameters M , $Gr\tau$, Grc, α, and ϕ on the wall shear stress c_f , heat transfer at the wall Nu and Sherwood number Sh.

The table shows that increasing the parameter M or α increases the wall shear stress as a result of increasing the resistive forces. The variation of $g'(0)$ and $h'(0)$ for various values of M is as the same as the effect on the wall shear stress, both the Nusselt and sherwood numbers increases as Hartmann's number increases.

It is clear that increasing M increases the magnitude of c_f, Nu and Sh, and the effect of M on the wall shear stress becomes more pronounced for higher values of M . The table also indicates that the magnitude of Nu decreases with increasing $Gr\tau$ or Grc and that for higher values of $Gr\tau$ or Grc, the effect on the wall shear stress is more pronounced.

5.0 Conclusion

The two-dimensional stagnation point flow of a viscous incompressible electrically conducting fluid with heat transfer has been studied. A numerical solution for the governing equations is obtained which allows the computation of the flow and heat transfer characteristics for various values of the Hartmann number M , the suction parameter α , heat generation/absorption coefficient ϕ and thermal and mass Grashof numbers $(Grt,\ Grc)$. The results indicate that increasing the parameter M or α ,decreases both the velocity and the thermal boundary layer thickness. On the other hand, the wall shear stress increases with increasing magnetic field. The results show that the heat transfer at the wall increases with increasing M , α , or ϕ .

Table 1: Variation of parameters M , $Gr\tau$, Grc, α, and ϕ on the wall shear stress c_f ,Nusseltnumber Nu and Sherwood number Sh

M	$Gr\tau$	Grc	α	ϕ	c_f	Nu	Sh
1	2	1	-1	-0.5	2.18691	0.30777	0.55363
1	2	1	0	-0.5	2.77323	0.53321	0.85398
1	2	1	1	-0.5	2.89664	0.92274	1.19820
0	2	1	-1	-0.5	2.14315	0.30768	0.55342
1	2	1	-1	-0.5	2.31686	0.30792	0.55482
2	2	1	-1	-0.5	2.80188	0.30792	0.56255
5	2	1	-1	-0.5	5.16311	0.30612	0.59961
8	2	1	-1	-0.5	7.93985	0.30462	0.62516
1	2	1	-1	-2	2.04162	0.03123	0.52604
1	2	1	-1	-1	2.12665	0.05003	0.54202
1	2	1	-1	0	2.26883	0.07353	0.56953
1	2	1	-1	1	2.22029	0.53281	0.53281
1	2	1	-1	2	1.90205	0.77924	0.52477
1	0	1	-1	-0.5	1.29438	0.31697	0.44754
1	1	1	-1	-0.5	1.74894	0.31214	0.50513
1	2	1	-1	-0.5	2.18691	0.30777	0.55363
1	4	1	-1	-0.5	3.02422	0.3	0.63321
1	2	0	-1	-0.5	1.80653	0.31079	0.51815
1	2	0.5	-1	-0.5	1.99939	0.30923	0.5366
1	2	1	-1	-0.5	2.18691	0.30777	0.55363
1	2	2	-1	-0.5	2.54865	0.30509	0.58435

Appendix

Destructive Chemical Reaction: Any type of combustion reaction could be considered "destructive". The type of combustion reaction often used in rocket engines.

Generative (pyrolysis) reactions: reaction that give more easily oxidized, gaseous fuels.

Thermal Grashof number: The GrashofnumberGrt is a dimensionless number which approximates the ratio of the buoyancy to viscous force acting on a fluid.

Mass Grashof number: is an analogous form of the thermal Grashof number used in cases of natural convection mass transfer problems.

Hartmann number is the ratio of electromagnetic force to the viscous force

Heat sink is a component that transfers heat generated within a solid material to a fluid medium, such as air or a liquid.

Heat source is a heat mechanism for heat generation in a system

Forced convection (flat plate, laminar flow): $Nu_{forced\ convection} \propto \mathrm{Re}^{\frac{1}{2}}$

Natural convection (vertical plate, laminar flow): $Nu_{natural convection} \propto Gr^{\frac{1}{4}}$

$Gr/\mathrm{Re}^2 < 0.1$: natural convection is negligible.

$Gr/\mathrm{Re}^2 > 10$: forced convection is negligible.

$0.1 < Gr/\mathrm{Re}^2 < 10$: forced and natural convection are not negligible.

The transition to turbulent flow occurs in the range $10^8 < Gr < 10^9$ for natural convection from vertical flat plates.

References

[1] K. Hiemenz, "Die Grenzschicht in einem in demgleichformingenFlussigkeitsstromeingetauchtengeradeKreiszylinder", *Dingler Polytechnic Journal*, 326, pp. 321–410, 1911

[2] J. T. Stuart, "The viscous flow near a stagnation point when the external flow has uniform vorticity," *Journal of Aerospace Science and Technology*, vol. 26, pp. 124–125, 1959.

[3] K. Tamada, “Two-dimensional stagnation-point flow impinging obliquely on a plane wall,” *Journal of the Physical Society of Japan*, vol. 46, no. 1, pp. 310–311, 1979.
[4] J. M. Dorrepaal, “An exact solution of the Navier-Stokes equation which describes nonorthogonalstagnation-point flow in two dimensions,” *Journal of Fluid Mechanics*, vol. 163, pp. 141–147, 1986.
[5] B. W. Beard and K. Walters, “Elastico-viscous boundary layer flows. I. Two-dimensional flow neara stagnation point,” *Mathematical Proceedings of the Cambridge Philosophical Society*, vol. 60, no. 3, pp.667–674, 1964.
[6] J. M. Dorrepaal, O. P. Chandna, and F. Labropulu, “The flow of a visco-elastic fluid near a point ofre-attachment,” *Zeitschrift f ¨urAngewandteMathematik und Physik*, vol. 43, no. 4, pp. 708–714, 1992.
[7] F. Labropulu, J. M. Dorrepaal, and O. P. Chandna, “Viscoelastic fluid flow impinging on a wall withsuction or blowing,” *Mech. Research Communications*, vol. 20, no. 2, pp. 143–153, 1993.
[8] T. Y. Na, *Computational Methods in Engineering Boundary Value Problems*, vol. 145 of *Mathematics inScience and Engineering*, Academic Press, New York, NY, USA, 1979.
[9] P. D. Ariel, “Hiemenz flow in hydromagnetics,” *ActaMechanica*, vol. 103, no. 1–4, pp. 31–43, 1994.
[10] Okedoye A. M., Faryola P. I. and Bello O. A. *MHD Flow of a Uniformly Stretched Vertical Permeable Surface under Oscillatory Suction Velocity.* J. Nigeria Association of Mathematical Physics pp 117 – 130, 2008
[11] M.F. White, *Viscous Fluid Flow.* New York: McGraw–Hill, (1991).